Monthly Notices
of the
ROYAL ASTRONOMICAL SOCIETY

MNRAS **485,** L109–L113 (2019)
Advance Access publication 2019 March 27

doi:10.1093/mnrasl/slz043

Precise optical timing of PSR J1023+0038, the first millisecond pulsar detected with Aqueye+ in Asiago

Luca Zampieri [1]★ Aleksandr Burtovoi [1,2] Michele Fiori,[1,3] Giampiero Naletto [1,3] Alessia Spolon,[1,3] Cesare Barbieri,[1,3] Alessandro Papitto[4] and Filippo Ambrosino[5]

[1]*INAF – Osservatorio Astronomico di Padova, Vicolo dell'Osservatorio 5, I-35122, Padova, Italy*
[2]*Centre of Studies and Activities for Space (CISAS) 'G. Colombo', University of Padova, Via Venezia 15, I-35131 Padova, Italy*
[3]*Department of Physics and Astronomy, University of Padova, Via F. Marzolo 8, I-35131, Padova, Italy*
[4]*INAF – Osservatorio Astronomico di Roma, Via Frascati 33, I-00076, Monteporzio Catone (RM), Italy*
[5]*INAF – Istituto di Astrofisica e Planetologia Spaziali, Via del Fosso del Cavaliere 100, I-00133 Rome, Italy*

Accepted 2019 March 19. Received 2019 March 15; in original form 2019 February 15

We report the first detection of an optical millisecond pulsar with the fast photon counter Aqueye+ in Asiago. This is an independent confirmation of the detection of millisecond pulsations from PSR J1023+0038 obtained with SiFAP at the Telescopio Nazionale Galileo. We observed the transitional millisecond pulsar PSR J1023+0038 with Aqueye+ mounted at the Copernicus telescope in 2018 January. Highly significant pulsations were detected. The rotational period is in agreement with the value extrapolated from the X-ray ephemeris, while the time of passage at the ascending node is shifted by 11.55 ± 0.08 s from the value predicted using the orbital period from the X-rays. An independent optical timing solution is derived over a baseline of a few days that has an accuracy of $\sim$0.007 in pulse phase ($\sim$12 μs in time). This level of precision is needed to derive an accurate coherent timing solution for the pulsar and to search for possible phase shifts between the optical and X-ray pulses using future simultaneous X-ray and optical observations.

Key words: accretion, accretion discs – stars: neutron – pulsars: general – pulsars: individual: PSR J1023+0038 – X-rays: binaries.

1 INTRODUCTION

Millisecond radio pulsars were discovered in 1982 (Alpar et al. 1982; Backer et al. 1982). The first confirmation of the long sought evolutionary link between these sources and accreting Low Mass X-ray Binaries (LMXBs) came in 1998 with the discovery of pulsations at 2.5 ms in SAX J1808.4-3658 (Wijnands & van der Klis 1998). This showed that old, low magnetic field pulsars are re-accelerated ('recycled') through mass and angular momentum transfer from a companion star in a previous LMXB phase.

However, it was only quite recently that direct evidence that some of these systems can swing between a rotation-powered millisecond pulsar phase and an accretion phase was gathered, thanks to the amazing discovery of an ordinary radio millisecond pulsar switching off and turning on as an accretion-powered, X-ray millisecond pulsar (PSR J1824-2452; Papitto et al. 2013). At present, we know other two systems that behave in a similar way: PSR J1023+0038 (Archibald et al. 2009) and PSR J1227-4853 (de Martino et al. 2010). These fast spinning, weakly magnetized neutron stars (NSs) are called transitional millisecond pulsars (tMSPs) and typically have low-mass companion stars ($\sim$0.5 $M_\odot$).

PSR J1023+0038, located at a distance of 1.37 ± 0.04 kpc (Deller et al. 2012), was initially classified as a Cataclysmic Variable (Bond et al. 2002). Subsequent observations carried out with the Green Bank Telescope showed that in 2007 the source was, in fact, a radio pulsar with a rotational period of 1.69 ms orbiting an $\sim$0.2 $M_\odot$ companion with a period of 4.75 h (Archibald et al. 2009). It was then realized that, between 2000 and 2001, the source had an accretion disc, which subsequently disappeared following the appearance of the radio millisecond pulsar. In 2013 June an inverse transition took place, with the disappearance of the radio pulses and the reappearance of the accretion disc, with a strong double-peaked Hα emission observed in the optical spectrum (Halpern et al. 2013; Patruno et al. 2014; Stappers et al. 2014). In the disc state the average optical and X-ray fluxes increase by a factor of $\sim$2–3 (Coti Zelati et al. 2014) and $\sim$10 (Stappers et al. 2014), respectively, the GeV γ-ray flux is 3–5 times higher (Torres et al. 2017), while only an upper limit exists on the TeV γ-ray flux (Aliu et al. 2016). As for the radio emission, bright

★ E-mail: luca.zampieri@inaf.it

© 2019 The Author(s)
Published by Oxford University Press on behalf of the Royal Astronomical Society

Downloaded from https://academic.oup.com/mnrasl/article/485/1/L109/5420503 by INAF Roma (Osservatorio Astronomico di Roma) user on 30 November 2020

continuum emission with a flat spectrum is observed, with radio flares occurring at certain phases (Deller et al. 2015; Bogdanov et al. 2018).

During the accretion phase significant X-ray variability is observed in PSR J1023+0038 on time-scales of tens of seconds. *XMM–Newton* observations show a puzzling trimodal behaviour in the 0.3–10 keV band. PSR J1023+0038 spends about 70–80 per cent of the time in a stable *high mode* with a X-ray luminosity $L_X \sim 7 \times 10^{33}$ erg s^{-1}. The source then unpredictably switches to a *low mode* with a much lower luminosity ($L_X \sim 10^{33}$ erg s^{-1}; Bogdanov et al. 2015; Campana et al. 2016; Coti Zelati et al. 2018), often correlated with enhancements of the radio emission (Bogdanov et al. 2018). Sporadic X-ray flaring episodes are also observed reaching luminosities $L_X \sim 10^{34}$ erg s^{-1} (*flaring mode*). Coherent X-ray pulsations at the NS spin period are detected only when the system is in the *high mode* (Archibald et al. 2015). The luminosity in this mode is lower than that of a typical LMXB. Notably, the spin rate of the pulsar during the accretion state is close to the value measured during the radio pulsar state (Jaodand et al. 2016).

Optical and infrared observations of PSR J1023+0038 revealed significant variability and flaring activity (Shahbaz et al. 2015, 2018; Hakala & Kajava 2018; Kennedy et al. 2018; Papitto et al. 2018), with an optical polarization degree up to ∼1 per cent (Baglio et al. 2016). A striking result coming from optical observations of PSR J1023+0038 was the discovery of millisecond optical pulsations with the spin period of the pulsar, produced in a region only a few tens of kilometres away from the NS (Ambrosino et al. 2017), most likely caused by an active rotation-powered pulsar even in the disc state.

The origin of the millisecond pulsations and the multiwavelength variability of PSR J1023+0038 in the disc state is a matter of lively debate at present. Several possibilities have been explored, from emission of a rotational powered pulsar (Coti Zelati et al. 2014; Li et al. 2014; Takata et al. 2014), to a pulsar in the propeller stage (Papitto, Torres & Li 2014; Papitto & Torres 2015), a pulsar accreting from a 'dead' disc (D'Angelo & Spruit 2012), or a pulsar switching between different regimes over short (∼10 s) time-scales (Linares 2014; Campana et al. 2016; Coti Zelati et al. 2018).

A crucial aspect to consider in all these models is the existence of millisecond optical pulsations. In order to understand the properties of these pulsations and their relation to the X-ray pulsations, it is important to foster the present observational framework and to increase the number and accuracy of the available optical measurements. In this context, we report the independent confirmation of the Ambrosino et al. (2017) detection of millisecond pulsations from PSR J1023+0038 with the fast photon counter Aqueye+ mounted at the Copernicus telescope in Asiago.

The plan of the paper is the following. In Section 2 we report the Aqueye+ observations of PSR J1023+0038 carried out in 2018 January, in Section 3 we show the results of our timing analysis, and in Section 4 we shortly discuss their potential impact in future simultaneous mutiwavelength campaigns.

2 OBSERVATIONS AND DATA ANALYSIS

We observed PSR J1023+0038 with Aqueye+ mounted at the Copernicus telescope in Asiago, Italy. Aqueye+ [1] is a fast photon counter with a field of view of few arcsec and the capability of time tagging the detected photons with sub-ns time accuracy (Barbieri et al. 2009; Naletto et al. 2013; Zampieri et al. 2015). A total of 30 acquisitions were performed between 2018 January 22 and 25, each lasting either ∼900 s or ∼1800 s. The overall on-source observing time is ∼44.1 ks. The log of the observations is shown in Table 1. The sky background was regularly monitored between on-target observations. The average background-subtracted rate of PSR J1023+0038 varied between ∼800 and ∼2000 c/s, mostly because of intrinsic source variability (flares).

Table 1. Log of the 2018 observations of PSR J1023+0038 taken with Aqueye+ at the 1.8 m Copernicus telescope in Asiago.

Observation ID	Start time (UTC)	Start time (MJD)	Duration (s)
20180122-011224	Jan 22[a] 00:20:10.2	58 140.014 007	899.4
20180122-012903	00:36:48.3	58 140.025 559	899.4
20180122-014725	00:55:10.3	58 140.038 314	899.4
20180122-020320	01:11:05.4	58 140.049 368	899.4
20180122-022214	01:29:59.5	58 140.062 494	899.4
20180122-023844	01:46:29.5	58 140.073 953	899.4
20180122-030122	02:09:07.6	58 140.089 671	1799.4
20180122-034854	02:56:39.7	58 140.122 682	1799.2
20180122-042617	03:34:02.9	58 140.148 645	1799.4
20180122-050133	04:09:20.0	58 140.173 148	1799.4
20180123-013839	Jan 23[a] 00:46:30.3	58 141.032 295	899.4
20180123-015619	01:04:10.4	58 141.044 565	899.4
20180123-021846	01:26:36.4	58 141.060 144	899.4
20180123-023447	01:42:38.5	58 141.071 279	899.4
20180123-025439	02:02:30.6	58 141.085 076	1799.4
20180123-033110	02:39:01.7	58 141.110 436	1799.4
20180123-040447	03:12:37.8	58 141.133 771	1799.3
20180123-044543	03:53:34.0	58 141.162 199	1799.4
20180124-023319	Jan 24[a] 01:41:14.4	58 142.070 306	1799.4
20180124-031307	02:21:02.5	58 142.097 946	1799.4
20180124-034843	02:56:39.6	58 142.122 681	1799.4
20180124-042332	03:31:27.8	58 142.146 849	1799.4
20180124-045838	04:06:33.9	58 142.171 226	1799.4
20180124-053343	04:41:39.0	58 142.195 590	1799.4
20180125-014934	Jan 25[a] 00:57:35.0	58 143.039 989	1799.4
20180125-024737	01:55:38.2	58 143.080 303	1799.4
20180125-034559	02:54:00.4	58 143.120 838	1799.4
20180125-042058	03:28:58.5	58 143.145 122	1799.4
20180125-045849	04:06:50.6	58 143.171 419	1799.4
20180125-054140	04:49:40.7	58 143.201 166	899.4

Note. Start times refer to the Solar system barycenter.
[a]Seeing: January 22 ∼2.9 arcsec, January 23 ∼2.9 arcsec, January 24 ∼2.0 arcsec, January 25 ∼2.3 arcsec.

The data reduction is performed with a dedicated software.[2] The whole acquisition and reduction chain ensure an absolute accuracy of ∼0.5 ns relative to UTC (Naletto et al. 2009). The photon arrival times are barycentered using TEMPO2 in TDB time units (Edwards, Hobbs & Manchester 2006; Hobbs, Edwards & Manchester 2006), using the position of Jaodand et al. (2016) (RA = $10^h23^m47.687198^s$, Dec. = $+00^o38'40.84551''$ at MJD 54995) and the JPL ephemerides DE405. We corrected for the motion of the NS along the orbit using the orbital period $P_{orb} = 0.198\,096\,3155$ d and projected semimajor axis $a = 0.343\,356$ light-seconds of Jaodand et al. (2016).

[1] https://web.oapd.inaf.it/zampieri/aqueye-iqueye/index.html

[2] QUEST v. 1.1.5, see Zampieri et al. (2015).

Downloaded from https://academic.oup.com/mnrasl/article/485/1/L109/5420503 by INAF Roma (Osservatorio Astronomico di Roma) user on 30 November 2020

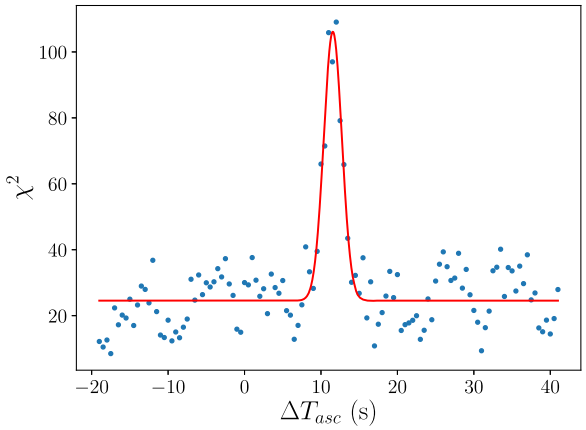

Figure 1. Epoch folding search of the time of passage at the ascending node for the 2018 January 25 Aqueye+ observation of PSR J1023+0038. Time is measured from the value of T_{asc} predicted using the orbital period from the X-ray ephemeris (Jaodand et al. 2016).

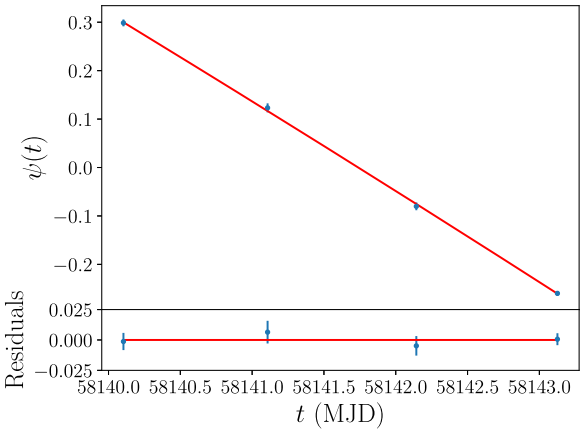

Figure 2. Phase drift $\psi(t)$ of PSR J1023+0038 with respect to a uniform rotation with period $P_{\rm init}$, fitted with a second-order polynomial (*solid* line). Time t is expressed in MJD. Residuals of the fit are shown in the bottom panel.

3 RESULTS

When PSR J1023+0038 transited to the accretion state, the time of passage of the pulsar at the ascending node $T_{\rm asc}$ showed an ∼20–30 s shift from the value measured during the radio pulsar phase. In addition to that, variations of a few seconds around an approximately sinusoidal modulation are observed (Jaodand et al. 2016; Papitto et al. 2019). Thus, following Ambrosino et al. (2017), we performed an accurate epoch folding search for the value of $T_{\rm asc}$ for our epoch by folding the corrected event lists of 2018 January 25, with the spin period extrapolated from the X-ray ephemeris (P_X = 1.687 987 4462 ms at t_0= 58 140.0 MJD; Jaodand et al. 2016) and with 16 bins per period. The maximum of the χ^2 is obtained for $T_{\rm asc}$ = 58 140.091 5932 ± 9 × 10^{-7} MJD, shifted by 11.55 ± 0.08 s from that predicted using the orbital period from the X-ray ephemeris (see Fig. 1). For this value of $T_{\rm asc}$ the variance of the pulse profile with respect to a constant ($\chi^2 = 100$ for 15 degrees of freedom) gives a probability $<10^{-14}$ that the pulsation is caused by a statistical fluctuation, corresponding to a detection significance of 7.7σ.

Using the actual value of $T_{\rm asc}$, we then performed a phase fitting of the Aqueye+ data, corrected for the binary motion, following the approach presented in previous works (Germanà et al. 2012; Zampieri et al. 2014; Spolon et al. 2019). We folded seperately the four nights of observations reported in Table 1 using as reference rotational period the value $P_{\rm init}$ = 1.687 987 440 ms and 16 bins per period. We detected the two peaks of the pulse profile in each night. They were fitted with the sum of two harmonically related sinusoids plus a constant (Ambrosino et al. 2017). To improve the accuracy of the measurement, we performed the fit fixing the separation $\Delta\phi$ and ratio ρ of the two sinusoids at the values obtained from fitting the pulse shape of the best observing night (2018 January 25): $\Delta\phi$ = 0.419, ρ = 1.27. The typical uncertainty on the phase measurement of each single night is ∼0.007 (or 12 μs).

The measured phases show a drift $\psi(t)$[3] with respect to a uniform rotation with period $P_{\rm init}$ (Fig. 2). We fitted it with a second-order polynomial and obtained the timing solution reported in Table 2. The rotational period ($P = 1/\nu_0$ = 1.687 987 445 96 ± 3.9 × 10^{-10} ms) is consistent within the uncertainties with the value extrapolated at t_0 = 581 40 MJD from the X-ray ephemeris (P_X = 1.687 987 446 202 ± 4 × 10^{-12} ms; Jaodand et al. 2016). Only an upper limit to the first derivative of frequency could be obtained. Timing noise is present at a level of ∼0.01 in phase. We note that additional terms accounting for the phase residuals induced by the orbital motion were not included in the fit because the reduced χ^2 of the second-order polynomial fit is smaller than unity (0.9) and because of the limited number of phase measurements available.

[3]As defined in Zampieri et al. (2014) and Spolon et al. (2019).

Table 2. Timing solution of the 2018 January Aqueye+ observations of PSR J1023+0038.

Timing solution of PSR J1023+0038 in 2018 January	
t_0	58140 MJD
ϕ_0	0.3186 ± 0.0073
ν_0	592.421 467 59 ± 1.4 × 10^{-7} Hz
$\lvert\dot{\nu}_0\rvert$	$<9 \times 10^{-13}$ Hz^2 [a]

Note. Uncertainties are calculated taking the square root of the diagonal terms in the covariance matrix of the fit.
[a]Upper limit estimated from the uncertainty on this parameter.

The final background-subtracted pulse shape obtained from folding all the 2018 January Aqueye+ observations with the timing solution reported in Table 2 and with 32 phase bins is shown in Fig. 3. A fit with the same model (two sinusoidal components plus a constant) adopted by Ambrosino et al. (2017) and Papitto et al. (2019) leads to consistent values of the parameters. The amplitudes of our two sinusoidal components are A_1 = 0.0033 ± 0.0002 and A_2 = 0.0046 ± 0.0002, and the phases are ϕ_1 = 0.671 ± 0.012 and ϕ_2 = 0.261 ± 0.004. The total fractional amplitude of the signal is $A = (A_1^2 + A_2^2)^{1/2}$ = 0.6 per cent. The variance of the pulse profile with respect to a constant (χ^2 = 440 for 31 degrees of freedom) gives a probability $<10^{-73}$ that the pulsation is caused by a statistical fluctuation, corresponding to a detection significance of 18.2σ.

We used the same model to investigate possible night-to-night variations of the pulse shape, keeping the relative phases of the two sinusoidal components fixed at the value inferred from the previous fit ($\Delta\phi$ = 0.41). The amplitudes of the two fitting sinusoids are in the interval A_1 = 0.002–0.005 and A_2 = 0.003–0.007. The corresponding curves are shown in Fig. 4. There are some differences in the quality of the pulse profiles in the various nights, but they do not appear to be caused by variations of the

Downloaded from https://academic.oup.com/mnrasl/article/485/1/L109/5420503 by INAF Roma (Osservatorio Astronomico di Roma) user on 30 November 2020

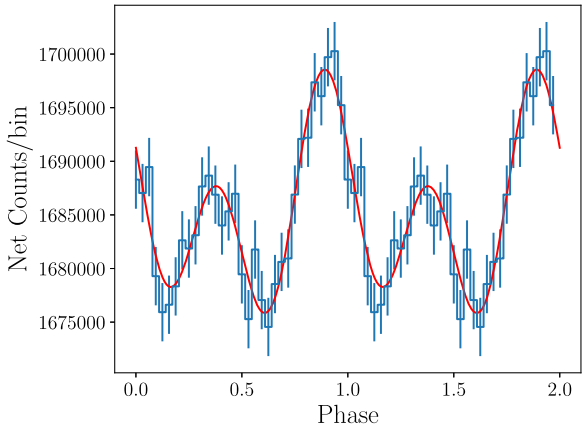

Figure 3. Background-substracted pulse shape of PSR J1023+0038 obtained folding all the Aqueye+ observations of 2018 January with the timing solution reported in Table 2 and with 32 bins per period. Two rotational phases are shown. The solid line shows the fit with two sinusoidal components plus a constant (model taken from Ambrosino et al. 2017).

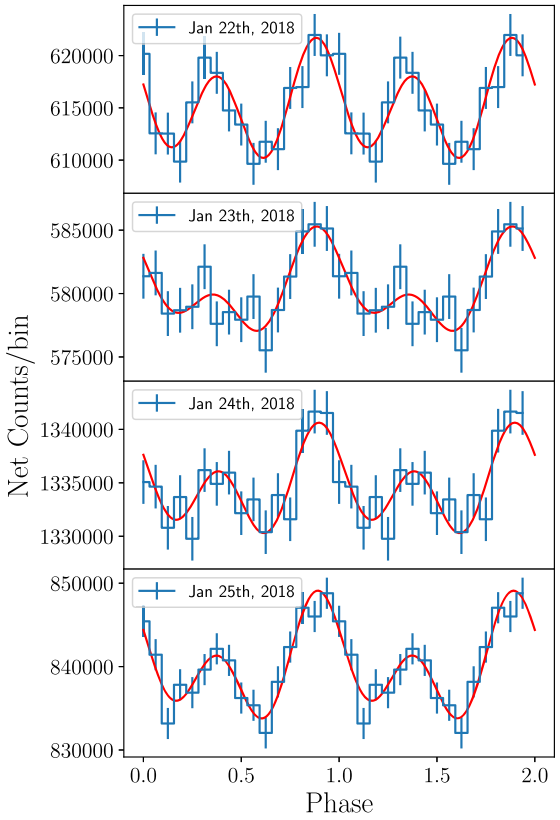

Figure 4. Background-substracted pulse shape of PSR J1023+0038 obtained folding each night of 2018 January with the timing solution reported in Table 2 and with 16 bins per period. Two rotational phases are shown. The solid lines show the fits with two sinusoidal components plus a constant (model taken from Ambrosino et al. 2017), where we keep the relative phases of the two sinusoidal components fixed ($\Delta\phi = 0.41$).

seeing conditions and/or depend in a straightforward way on the average source rate. Indeed, the night with the best seeing and the highest background-subtracted average rate (January 24; see Table 1 and Fig. 4) is not the one with the best pulse quality. Despite the different quality of the pulse profiles, we find evidence that the height of the second peak (defined as maximum minus minimum of the corresponding peak of the fitting function) varies significantly compared to that of the first peak. From January 22 through January 25, the ratio of the two peaks is 0.68 ± 0.07, 0.35 ± 0.08, 0.56 ± 0.09, and 0.49 ± 0.05, respectively.

4 DISCUSSION AND CONCLUSIONS

We analyzed the 2018 January Aqueye+ observations of PSR J1023+0038 and detected, for the first time with Aqueye+, a highly significant millisecond pulsation. The rotational period ($P = 1/\nu_0 = 1.687\,987\,445\,96 \pm 3.9 \times 10^{-10}$ ms) is consistent within the uncertainties with the value extrapolated from the X-ray ephemeris of Jaodand et al. (2016) and the properties of the pulse shape are similar to those reported by Ambrosino et al. (2017). Night-to-night variations of the pulse shape are observed, with the height of the second peak varying significantly (compared to that of the first peak).

The accuracy of our timing and acquisition system allowed us to derive an independent timing solution for PSR J1023+0038 and to measure its absolute rotational phase with high accuracy (∼12 μs) using four consecutive observing nights. This level of accuracy is needed to search for possible phase shifts between the optical and X-ray pulses, as done for other optical pulsars as the Crab pulsar (e.g. Zampieri et al. 2014) or the Vela pulsar (Spolon et al. 2019). For the Crab pulsar, the optical peak clearly leads the radio peak, but is in phase with the X-ray one (within ∼0.003). A similar evidence for a phase alignment of the optical and X-ray peaks that correspond to the radio peak is found in the Vela pulsar. If the optical and X-ray peaks of PSR J1023+0038 are in phase, this would then suggest that the emission mechanism is the same, likely a rotation-powered pulsar. Conversely, finding a significant phase shift bewteen the optical and X-ray peaks would provide independent evidence that a different emission mechanism is at work. For PSR J1023+0038 an accuracy of ∼12 μs, as that obtained from our timing solution, guarantees to pinpoint a phase shift as small as ∼0.01.

Other optical measurements of the absolute rotational phase of PSR J1023+0038 could be affected by systematic errors related to the drift of the internal clock of the acquisition system. To compensate for this effect, Ambrosino et al. (2017) apply a linear correction to the photon arrival times of their event lists. This linear correction is calibrated comparing the time of arrival of the main peak of the Crab pulsar from an optical observation taken in 2016 February with that reported in the Jodrell Bank monthly ephemeris[4] (Lyne, Pritchard & Graham-Smith 1993). Ambrosino et al. (2017) find that the optical peak leads the radio one by ∼180 μs, in agreement with previous findings (e.g. Germanà et al. 2012; Zampieri et al. 2014). However, the Jodrell Bank ephemeris contains monthly averages of the phase measurements and can be affected by errors of ≈100 μs. For 2016 February, the reported error is 70 μs, but weekly phase excursions around the monthly ephemeris could be as large as ∼50–100 μs, as shown in Čadež et al. (2016). For this reason, considering the accuracy of our timing solution, simultaneous optical measurements of the absolute phase of PSR J1023+0038 with Aqueye+ at Copernicus are desirable. They can serve not only because of their intrinsic scientific value, but also as calibrators for observations taken with other optical facilities.

As far as the X-ray observations are concerned, their timing accuracy depends on the satellite and the instrument. The EPIC-

[4] http://www.jb.man.ac.uk/pulsar/crab.html

Downloaded from https://academic.oup.com/mnrasl/article/485/1/L109/5420503 by INAF Roma (Osservatorio Astronomico di Roma) user on 30 November 2020

pn instrument onboard *XMM–Newton* in the timing mode has an uncertainty of 48 μs on the absolute timing and a clock drift of $<10^{-8}$ ss^{-1} (Martin-Carrillo et al. 2012). The clock drift appears to be sufficiently small not to lead to a significant smearing of the pulse profile of PSR J1023+0038 during a 30 ks long observation (Jaodand et al. 2016). However, the absolute error may lead to a non-negligible uncertainity in the measurement of the phase shift with respect to other measurements at the level of 0.03. Simultaneous Aqueye+ observations could then be used to determine the optical-X-ray shift (if it is $\gtrsim 0.03$) or to cross-calibrate the optical and X-ray measurements.

Unfortunately, because no X-ray observations were performed at the time of the Aqueye+ observations, we can neither measure directly the X-ray-optical time delay using the present data set, nor can we select *high* and *low mode* time intervals to improve the significance of our measurements. However, future simultaneous multiwavelength campaigns in synergy with X-ray telescopes and with SiFAP at TNG will certainly allow us to perform an accurate measurement of the relative shift between the X-ray and optical peaks in the pulse shape of PSR J1023+0038. This type of measurements provide significant constraints to the geometry of the emission region and, ultimately, to the physical mechanism producing the optical and X-ray pulses.

ACKNOWLEDGEMENTS

We thank the referee for the useful comments. We would like to thank M. Barbieri, P. Ochner, L. Lessio, and all the technical staff at the Asiago Cima Ekar Observatory for their valuable operational support. This Letter is based on observations collected at the Copernicus telescope (Asiago, Italy) of the INAF-Osservatorio Astronomico di Padova. We acknowledge financial contribution from the grant ASI/INAF n. 2017-14-H.O (projects 'High-Energy observations of Stellar-mass Compact Objects: from CVs to Ultra-luminous X-Ray Sources' and 'Understanding the x-ray variabLe and Transient Sky (ULTraS)') and grant ASI/INAF n. I/037/12/0. This research made use also of the following PYTHON packages: MATPLOTLIB (Hunter 2007), NUMPY (van der Walt, Colbert & Varoquaux 2011), and ASTROPY (Astropy Collaboration 2013).

REFERENCES

Aliu E. et al., 2016, ApJ, 831, 193
Alpar M. A., Cheng A. F., Ruderman M. A., Shaham J., 1982, Nature, 300, 728
Ambrosino F. et al., 2017, Nat. Astron., 1, 854
Archibald A. M. et al., 2009, Science, 324, 1411
Archibald A. M. et al., 2015, ApJ, 807, 62
Astropy Collaboration, 2013, A&A, 558, A33
Backer D. C., Kulkarni S. R., Heiles C., Davis M. M., Goss W. M., 1982, Nature, 300, 615
Baglio M. C., D'Avanzo P., Campana S., Coti Zelati F., Covino S., Russell D. M., 2016, A&A, 591, A101
Barbieri C. et al., 2009, J. Mod. Opt., 56, 261
Bogdanov S. et al., 2015, ApJ, 806, 148
Bogdanov S. et al., 2018, ApJ, 856, 54
Bond H. E., White R. L., Becker R. H., O'Brien M. S., 2002, PASP, 114, 1359
Campana S., Coti Zelati F., Papitto A., Rea N., Torres D. F., Baglio M. C., D'Avanzo P., 2016, A&A, 594, A31
Coti Zelati F., Campana S., Braito V., Baglio M. C., D'Avanzo P., Rea N., Torres D. F., 2018, A&A, 611, A14
Coti Zelati F. et al., 2014, MNRAS, 444, 1783
Čadež A., Zampieri L., Barbieri C., Calvani M., Naletto G., Barbieri M., Ponikvar D., 2016, A&A, 587, A99
Deller A. T. et al., 2012, ApJ, 756, L25
Deller A. T. et al., 2015, ApJ, 809, 13
de Martino D. et al., 2010, A&A, 515, A25
D'Angelo C. R., Spruit H. C., 2012, MNRAS, 420, 416
Edwards R. T., Hobbs G. B., Manchester R. N., 2006, MNRAS, 372, 1549
Germanà C. et al., 2012, A&A, 548, A47
Hakala P., Kajava J. J. E., 2018, MNRAS, 474, 3297
Halpern J. P., Gaidos E., Sheffield A., Price-Whelan A. M., Bogdanov S., 2013, Astron. Telegram, 5514
Hobbs G. B., Edwards R. T., Manchester R. N., 2006, MNRAS, 369, 655
Hunter J. D., 2007, Comput. Sci. Eng., 9, 90
Jaodand A., Archibald A. M., Hessels J. W. T., Bogdanov S., D'Angelo C. R., Patruno A., Bassa C., Deller A. T., 2016, ApJ, 830, 122
Kennedy M. R., Clark C. J., Voisin G., Breton R. P., 2018, MNRAS, 477, 1120
Li K. L., Kong A. K. H., Takata J., Cheng K. S., Tam P. H. T., Hui C. Y., Jin R., 2014, ApJ, 797, 111
Linares M., 2014, ApJ, 795, 72
Lyne A. G., Pritchard R. S., Graham-Smith F., 1993, MNRAS, 265, 1003
Martin-Carrillo A. et al., 2012, A&A, 545, A126
Naletto G. et al., 2009, A&A, 508, 531
Naletto G. et al., 2013, in Meyers R. E., Shih Y., Deacon K. S., eds, Proc. SPIE Conf. Ser. Vol. 8875, Quantum Communication and Quantum Imaging XI, SPIE, Bellingham, p. 88750D
Papitto A., Torres D. F., 2015, ApJ, 807, 33
Papitto A., Torres D. F., Li J., 2014, MNRAS, 438, 2105
Papitto A. et al., 2013, Nature, 501, 517
Papitto A. et al., 2018, ApJ, 858, L12
Papitto A. et al., 2019, ApJ, submitted
Patruno A. et al., 2014, ApJ, 781, L3
Shahbaz T., Dallilar Y., Garner A., Eikenberry S., Veledina A., Gandhi P., 2018, MNRAS, 477, 566
Shahbaz T. et al., 2015, MNRAS, 453, 3461
Spolon A., Zampieri L., Burtovoi A., Naletto G., Barbieri C., Barbieri M., Patruno A., Verroi E., 2019, MNRAS, 482, 175
Stappers B. W. et al., 2014, ApJ, 790, 39
Takata J., Leung G. C. K., Tam P. H. T., Kong A. K. H., Hui C. Y., Cheng K. S., 2014, ApJ, 790, 18
Torres D. F., Ji L., Li J., Papitto A., Rea N., de O na Wilhelmi E., Zhang S., 2017, ApJ, 836, 68
van der Walt S., Colbert S. C., Varoquaux G., 2011, Comput. Sci. Eng., 13, 22
Wijnands R., van der Klis M., 1998, Nature, 394, 344
Zampieri L. et al., 2014, MNRAS, 439, 2813
Zampieri L. et al., 2015, in Prochazka I., Sobolewski R., James R. B., eds, Proc. SPIE Conf. Ser. Vol. 9504, Photon Counting Applications 2015, SPIE, Bellingham, p. 95040C

This paper has been typeset from a TEX/LATEX file prepared by the author.

Downloaded from https://academic.oup.com/mnrasl/article/485/1/L109/5420503 by INAF Roma (Osservatorio Astronomico di Roma) user on 30 November 2020